Tendon Fascicles Exhibit a Linear Correlation Between Poisson's Ratio and Force During Uniaxial Stress Relaxation

Shawn P. Reese

Jeffrey A. Weiss[1]
e-mail: jeff.weiss@utah.edu

Department of Bioengineering,
University of Utah,
Salt Lake City, UT 84112

*The underlying mechanisms for the viscoelastic behavior of tendon and ligament tissue are poorly understood. It has been suggested that both a flow-dependent and flow-independent mechanism may contribute at different structural levels. We hypothesized that the stress relaxation response of a single tendon fascicle is consistent with the flow-dependent mechanism described by the biphasic theory (Armstrong et al., 1984, "An Analysis of the Unconfined Compression of Articular Cartilage," ASME J. Biomech. Eng., **106**, pp. 165–173). To test this hypothesis, force, lateral strain, and Poisson's ratio were measured as a function of time during stress relaxation testing of six rat tail tendon fascicles from a Sprague Dawley rat. As predicted by biphasic theory, the lateral strain and Poisson's ratio were time dependent, a large estimated volume loss was seen at equilibrium and there was a linear correlation between the force and Poisson's ratio during stress relaxation. These results suggest that the fluid dependent mechanism described by biphasic theory may explain some or all of the apparent viscoelastic behavior of single tendon fascicles.* [DOI: 10.1115/1.4023134]

Keywords: tendon, stress relaxation, Poisson's ratio, biphasic, viscoelasticity

Introduction

The viscoelastic behavior of ligaments and tendons is thought to play an important role in the normal function of these tissues. The time and rate dependent behaviors are manifested as stress relaxation, creep, and hysteresis. The viscoelastic properties dissipate energy and thus may protect the tissue from damage [1]. Experimentally observed changes in viscoelastic behavior in damaged and diseased tissue highlights the importance of understanding the rate and time dependence [2,3]. However, the exact mechanisms giving rise to the viscoelastic behavior of ligaments and tendons at the continuum level remain unclear.

Discerning the source of this behavior is complicated by the multiscale structural organization and high level of hydration in these tissues. Stress relaxation mechanisms may be both flow dependent and flow independent, and may occur at different structural levels [4–9]. Rate dependent behavior has been observed at the fibril level, fiber level, fascicle level, and tissue level [4,8,10,11]. This study focused on the viscoelastic behavior at the fascicle level, and more specifically, the flow-dependent mechanisms. Understanding the fascicular response is fundamental to understanding the macroscopic tissue response, and the fascicle level was deemed a prudent starting point in understanding the multiscale viscoelastic behavior of tendon and ligament tissue.

It has been suggested that biphasic theory may explain the apparent viscoelastic behavior of single fascicles [9]. According to biphasic theory, apparent viscoelasticity is a result of energy dissipated from fluid flux through a porous solid phase [12,13]. This fluid flux is driven by volumetric strain, governed by the Poisson's effect of the elastic solid phase. During stress relaxation, biphasic theory predicts a time dependent lateral contraction, which would be manifested experimentally as a time dependent Poisson's ratio. Furthermore, biphasic theory predicts that the instantaneous force during relaxation should be proportional to the instantaneous lateral contraction. These observations motivated our hypothesis that during stress relaxation, single fascicles will display a time dependent lateral strain and Poisson's ratio, a large volume loss at equilibrium and a linear correlation between force and Poisson's ratio. To test this hypothesis, the force, transverse strain, and Poisson's ratio were measured in single rat tail tendon (RTT) fascicles during stress relaxation testing.

Materials and Methods

Rat tail tendon fascicles were chosen for this study. In addition to their use in many previous studies of tendon mechanics [14–18], tendon fascicles are easy to obtain, have a large aspect ratio that is conducive to obtaining homogenous strains and have nearly cylindrical cross sections that aid in measuring transverse strain. Rat tail tendons were obtained from a single, freshly sacrificed Sprague Dawley rat, placed in gauze, moistened using phosphate buffered saline, and frozen for future testing. On the day of testing, tendons were allowed to thaw at room temperature and single fascicles were removed from the tendons. A total of six samples were isolated from six different tendons. Each sample was cut to a length of approximately 20 mm. Fascicle diameters were approximately 250 μm, providing an aspect ratio of 80:1. Samples were attached to a mini materials test machine using custom clamps and tested in a PBS bath at room temperature. During pilot testing it was observed that the fascicles appeared to rotate a small amount (less than a quarter turn) during constant strain rate testing, which is consistent with previous observations [17]. Since both clamps were fixed, this was not true rotation. Because of this apparent rotation, surface markers would rotate with respect to the camera focal plane. To ensure a constant profile for tracking axial strain, small black beads with a hole drilled in the center were slid onto the tendon fascicle and affixed 10 mm apart using cyanoacrylate gel. The beads served as fiducials to track axial strain. The use of bead markers ensured that each marker had a consistent profile in the presence of rotation. Digital images of the sample were acquired at a rate of 2.0 Hz (resolution = 1024 × 1360 pixels) using a digital motion analysis camera (GC1350, Allied Vision Technologies, Stadtroda, Germany) and saved for strain analysis. Force was recorded using a 10 N load cell and the displacements and image acquisition was controlled using a custom LabVIEW program. A prestrain was induced in the samples by applying a 0.4 N tare load. Preliminary experiments demonstrated that this load was adequate to remove slack in the sample and to prevent excessive rotation during testing. Samples were preconditioned by applying 10 cycles of a triangular displacement profile to 3.0% clamp-to-clamp strain at a strain rate of 0.5%/s. Samples were allowed to recover for 10 min after preconditioning [19]. Stress relaxation testing was then performed, with a ramping strain rate of 0.5%/s, a maximum strain of 3%, and a relaxation time of 300 s. The force at 300 s was within 95% of the equilibrium force. Therefore, 300 s was chosen as the end point to reduce the required storage space for the digital video data.

A custom Matlab program was used to analyze strain from the images acquired during the ramping phase and stress relaxation. Images were binarized using a threshold value of 0.15, and the outline of the sample, defined as the tissue between the two bead markers, was segmented. A sensitivity study was performed on

[1]Corresponding author.

Contributed by the Bioengineering Division of ASME for publication in the Journal of Biomechanical Engineering. Manuscript received May 16, 2012; final manuscript received November 12, 2012; accepted manuscript posted December 8, 2012; published online February 11, 2013. Editor: Beth Winkelstein.

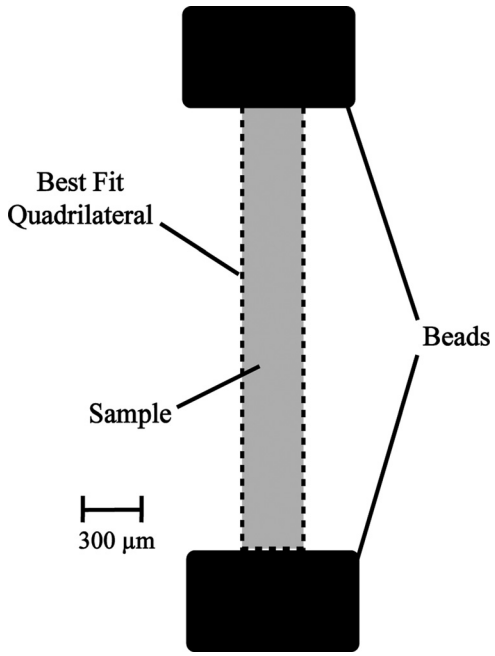

Fig. 1 Sample schematic. A typical image used for calculating axial strain, transverse strains, and Poisson's ratio. The sample, marker beads, and the best fit quadrilateral are indicated.

the threshold value and it was found that a range of threshold values (ranging from 0.1 to 0.2) yielded similar results. Therefore the mean value of this range (0.15) was chosen. A quadrilateral was fit to the segmented image using a global optimization routine, based on the pattern search algorithm in Matlab's optimization toolbox (Fig. 1). The deformation gradient for each time point was computed from the nodes of the best fit quadrilateral:

$$F_{iJ} = \sum_{a=1}^{4} x_{a,i} \frac{\partial N_a}{\partial X_J} \tag{1}$$

where $\partial N_a/\partial X_J$ is the derivative of the ath shape function with respect to the reference configuration and $x_{a,i}$ is the deformed nodal coordinates for the ath node [20]. The deformation gradient was then used to compute the engineering strain along the fiber direction (e_f) and the transverse direction (e_t). The Poisson's ratio in the fiber plane υ was computed using the standard formula $\upsilon = -e_t/e_f$. In order to validate the methodology, a white rubber cord with a similar diameter to the fascicles was tested. The mean Poisson's ratio measured for the rubber samples was close to 0.5, which is the Poisson's ratio for incompressible rubber at small strains [21].

To minimize the effects of rotation, analysis was performed for strains larger than the transition strain (the point where the exponential region becomes linear), as rotation of the fascicle generally ceased by this point. The transition strain was found by performing a nonlinear curve fit to a piecewise exponential and linear function described previously [22]:

$$f(\lambda) = \begin{Bmatrix} 0 & \lambda \le 1 \\ c_1\left(e^{c_2(\lambda-1)} - 1\right) & \lambda < \lambda^* \\ c_3\lambda + c_4 & \lambda \ge \lambda^* \end{Bmatrix} \tag{2}$$

where f is the force, λ is the applied clamp stretch along the fiber direction, λ^* is the transition stretch, and $c_1 - c_4$ are material coefficients. The fascicle length and width at the transition strain was chosen as the reference configuration (Fig. 2). The mean values and standard deviations for the force, axial strain, transverse strain, and Poisson's ratio were computed for all samples at all

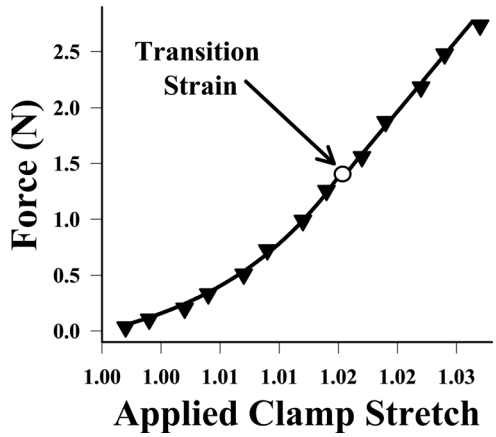

Fig. 2 Computing transition strain. A typical curve of force versus applied clamp stretch during the ramping phase is shown, where black triangles represent the data points, the solid line represents the nonlinear curve fit, and an empty circle represents the transition strain.

time points. The force and Poisson's ratio from the stress relaxation were normalized to allow simultaneous comparison of all samples. The normalization was performed by first subtracting the minimum value obtained during the relaxation from the original data, yielding a data set with a minimum value of zero. The maximum value of the resulting data set was then used for normalization, yielding a data set that ranged from zero to one. A linear correlation was performed between the normalized force and normalized Poisson's' ratio using the data points for all samples. To provide equal weight to points during stress relaxation, the data were resampled logarithmically.

Results

The mean transverse strain was negative during stress relaxation and decreased with time (Fig. 3, top), while the mean Poisson's ratio was positive and increased with time (Fig. 4, top). The mean Poisson's ratio during the initial ramping phase (averaged over all samples) was 0.70 ± 0.52, and it increased to a mean value of 4.26 ± 1.53 by the end of stress relaxation. This behavior was qualitatively similar to the decrease in the force measured during relaxation (Fig. 4 bottom). A plot of the normalized force versus the normalized Poisson's ratio for all samples revealed a linear relationship (Fig. 5, $m = -1.05$, $R^2 = 0.85$). The linear correlation was significant with a p value of $\alpha < 0.0001$. It was assumed that the sample cross section was circular. The equilibrium volume ratio was computed from the mean axial and transverse strains and had a value of 0.836 ± 0.065, which corresponds to a mean volume loss of $16.4 \pm 6.5\%$. The axial tissue strain, measured optically, was constant in time and correlated linearly with the applied clamp strain by a value of $75\% \pm 12\%$ (Fig. 3, bottom). A linear fit was performed on the optically measured fiber strain versus time and had a slope of zero and a y intercept of 1.13%. The transition strain computed from the nonlinear curve fits of the force and applied clamp stretch and had a value of $1.40 \pm 0.26\%$.

Discussion

As hypothesized, the volumetric behavior of RTT during stress relaxation was time dependent. This was manifested as a decrease in lateral strain and a corresponding increase in Poisson's ratio with relaxation time. The mean Poisson's ratios for all times were in excess of the isotropic limit of 0.5, which is indicative of volume loss during uniaxial tensile testing. Assuming a cylindrical cross section, the mean volume loss at the end of testing was 16.4%, signifying a time dependent fluid exudation. This is

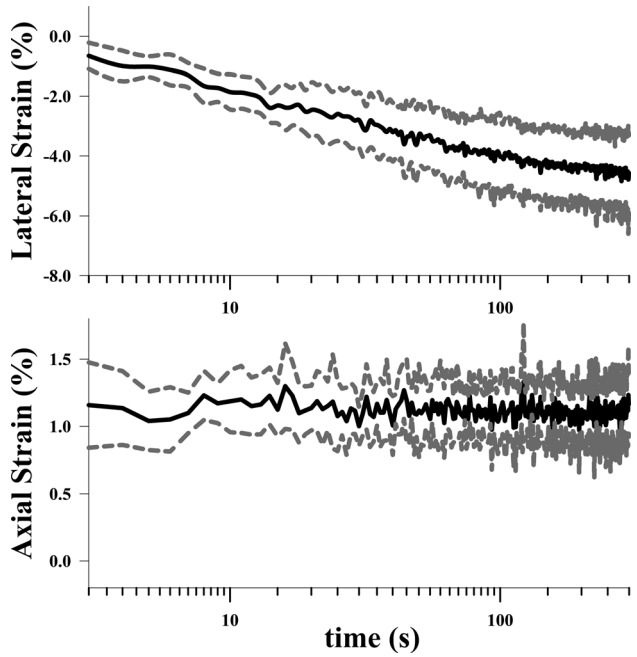

Fig. 3 Lateral and axial strain versus time. (Top) Transverse strain versus time (log scale) for all samples. (Bottom) Axial strain versus time (log scale) for all samples. A linear fit of the axial tissue strain resulted in a negligible slope, indicating that it was constant during relaxation. In both plots the solid line is the mean value (averaged over all samples) while the dashed line represents the standard deviation for each time point. Note that all strains were measured using the transition strain as the reference position.

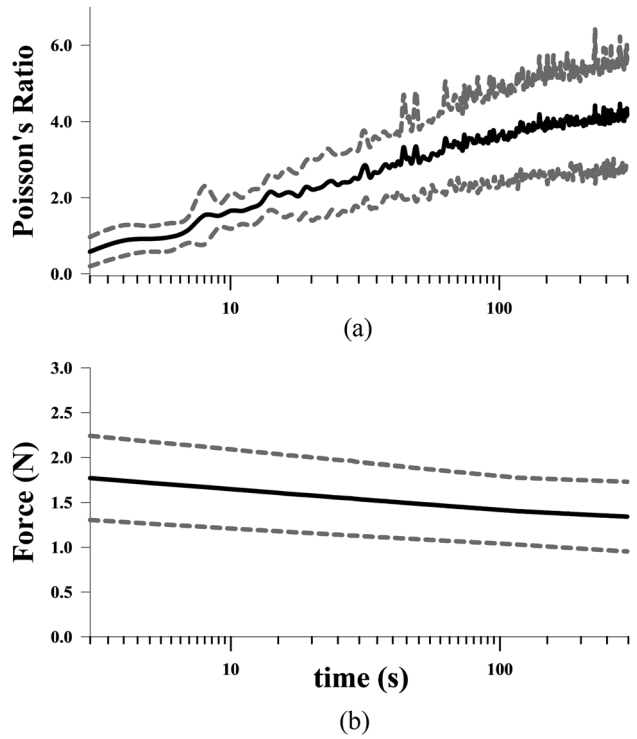

Fig. 4 Poisson's ratio and force versus time. (Top) Poisson's ratio versus time (log scale) for all samples. (Bottom) Force versus time (log scale) for all samples. The solid line is the mean value (averaged over all samples) while the dashed line represents the standard deviation for each time point.

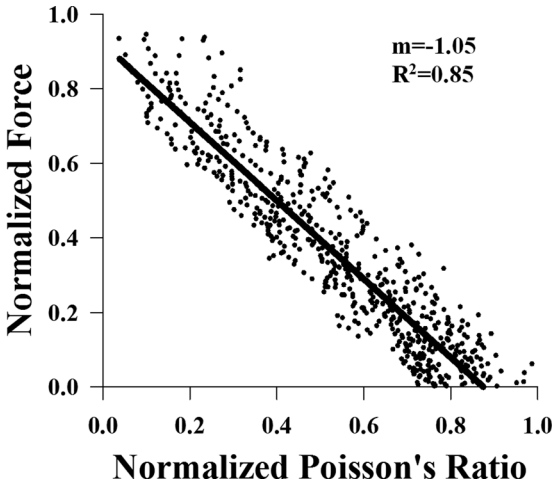

Fig. 5 The normalized force plotted against the normalized Poisson's ratio for all data points. Note that the data were logarithmically sampled in time to provide an equal distribution of points throughout the entire data range. The data points are the black dots and the best fit is represented by a solid black line. The slope and R^2 value are displayed in the upper right hand corner.

supported by previous studies that have reported fluid exudation during tensile loading [23–25]. The average Poisson's ratio during the ramp phase was 0.70, which indicates nearly incompressible behavior during fast loading, as predicted by biphasic theory. The average Poisson's ratio at the end of stress relaxation was 4.26, indicating anisotropic elastic behavior with a large volume loss. The correlation between the Poisson's ratio and force during relaxation revealed an intrinsic connection between volumetric behavior and stress during the relaxation processes. These results agree with predictions from biphasic theory and suggest some or all of the apparent viscoelastic response may be explained by flow-dependent mechanisms. This result is highly relevant, as fluid movement has been implicated in nutrient transport and mechanotransduction and may be fundamentally important in the behavior of fascicles in normal tissues [6,9,26,27].

The results from this study are supported by previous biphasic fits of the material behavior of collagenous tissues in the literature. Transversely isotropic biphasic fits were performed on incremental stress relaxation data of mouse tail fascicles, and excellent fits were obtained [9]. The study predicted Poisson's ratio's ranging from 2.0 to 2.4, which compares reasonably to the measured value of 4.26 in the current study. Large Poisson's ratios were also reported for sheep flexor tendon ($\nu = 2.98 \pm 2.59$) [28], capsular ligament tissue ($\nu = 2.0 \pm 1.9$) [29], and meniscus ($\nu = 2.13 \pm 1.27$) [30], suggesting that a large volumetric loss during tensile loading is an intrinsic material characteristic of these tissues. Although previous studies have characterized the stress response of tendon fascicles during relaxation [31,32], this is the first study to characterize the lateral strain and Poisson's ratio during relaxation.

Apparent rotation of the fascicles was observed during the ramping phase of tensile elongation below the transition strain, as previously observed [17]. This suggests the presence of a helical organization within the fascicle. Micromechanical models of helical structures within tendon and ligament suggest the presence of helical twisting, which may be responsible for the large experimentally observed Poisson's ratios [33]. Evidence for helical organization has been reported in histological studies on tendon and ligament [34–37]. Although attempts were made to measure the apparent rotation, the 2D nature of the images precluded accurate estimates. In addition to apparent rotation, the fascicle was also observed to slightly change shape within the toe region. Further study of this behavior may yield relevant information regarding the structure-function behavior of single fascicles.

The primary limitation of this study was that the analysis was restricted to strains exceeding the transition strain. Since the fiber and transverse strain could not be calculated within the toe region, a systematic offset was introduced into the calculation of the Poisson's ratio. The actual Poisson's ratio would be calculated using $\upsilon = -(e_t^0 - e_t^*)/(e_t^0 - e_t^*)$, where e_t^0 and e_a^0 are the unknown transverse and fiber strains within the toe region and e_t^* and e_a^* are the strains measured relative to the transition strain and reported. In the analysis presented in this study, e_t^0 and e_a^0 were taken to be zero, which is not actually the case. If it is assumed that the Poisson's ratio in the toe region is the same as that of the linear region and that the axial strain rate within the toe region is the same as within the linear region, the strains within the toe region can be estimated. When this analysis is performed, the Poisson's ratio versus time curve (Fig. 4) is scaled by a constant factor of 0.44. The shape (and resulting slope of the best fit line in Fig. 5) remains the same and the Poisson's ratio during the linear portion of the linear phase in unchanged, but the equilibrium Poisson's ratio has a value of 1.87 ± 0.88. This value is very close to the values estimated from biphasic curve fits by Yin et al. [9]. In order to obtain measured values of strain within the toe region, a more sophisticated approach to measuring transverse strain will be needed. More specifically, a method for reconstructing the 3D cross section of the fascicle will be required to compensate for the strain artifacts induced by fascicle rotation and shape change. It would have been desirable to fit biphasic models to the stress data and determine their capability to predict transverse strain. However, the use of a single strain level combined with material nonlinearity made this infeasible. Incremental stress relaxation testing could address part of this issue and we hope to purse these studies in the future.

Another limitation of this study was noise in the strain data and thus measurements for Poisson's ratio due to the resolution of the camera ($\sim$1 μm/pixel) and the size of the sample within the field of view. Given the typical width of the sample ($\sim$250 pixels), an error in the segmentation by a single pixel resulted in an error in the Poisson's ratio of $\sim$0.3, which is comparable to the error in the data. The segmentation errors were dependent on image quality, which was affected by convection currents in the PBS bath. A further limitation of this study is the use of fascicles from a single rat tail. In pilot studies the same qualitative behavior was observed in fascicles obtained from different animals. Therefore, we do not expect that analysis of samples from different animals would significantly change the conclusions. Finally, it was assumed that the fascicle had a cylindrical shape. Microscopy suggests that in the relaxed state, fascicles have a triangular shape [15]. However, previous work has demonstrated that the assumption of a cylindrical shape provides a useful approximation [9,31]. Although this has yet to be demonstrated, qualitative observations showed that fascicles may take on a more cylindrical shape in the linear region of the stress-strain curve. Again, a more sophisticated 3D system for shape measurement could address this issue. Finally, cross sectional area measurements were not made as part of this study. Thus force relaxation, not stress relaxation, was reported. Since the data were pooled across samples for the regression analyses, the stress would be related to the force by a linear constant (namely, the reciprocal of the average cross sectional area). Thus, the correlation between force and Poisson's ratio in Fig. 5 would be unaffected by converting force to stress.

With an understanding of how single fascicles behave, the question as to how this behavior translates to whole tissue behavior naturally arises. Given that experimental measurements of the Poisson's ratio in whole tissue preparations are also large [28,29], it can be assumed that adjacent fascicles are mechanically coupled in such a way as to generate a large macroscopic volumetric response. However, elucidating the mechanisms of fluid flux at the macroscopic level is an open question. It is possible (as previously suggested [9]) that the primary resistance to fluid flux occurs at the fascicle level and that resistance to fluid flow between fascicles and out of the tissue may be minimal. It is also possible that fluid cannot freely flow between fascicles, which would suggest the presence of flow-dependent viscoelastic mechanisms at different structural levels. Measuring the volumetric response during stress relaxation of whole tissue preparations will help to elucidate these mechanisms.

This study highlights an important connection between the axial stress and the Poisson's ratio during stress relaxation testing of RTT. This may provide evidence for the biphasic origins of tissue viscoelasticity and suggests that the time dependent axial stress behavior is intrinsically linked to the lateral relaxation of the tissue. However, the authors note that these results are not sufficient to conclude that the tissue is behaving in a biphasic manner. Further experiments could be performed to determine the presence and magnitude of fluid flow out of fascicles during tensile loading. Furthermore, additional work is needed to determine the relative contribution of the solid and fluid phase to the apparent viscoelastic behavior of single tendon fascicles. Curve fitting of poroviscoelastic models may be a useful means for elucidating these mechanisms and should be a focus of future research [38–42].

Acknowledgment

Financial support from NIH Grant Nos. R01AR053344 and R01GM083925 is gratefully acknowledged.

References

[1] Bonifasi-Lista, C., Lake, S. P., Small, M. S., and Weiss, J. A., 2005, "Viscoelastic Properties of the Human Medial Collateral Ligament Under Longitudinal, Transverse and Shear Loading," J. Orthop. Res., **23**, pp. 67–76.
[2] Woo, S. L., Debski, R. E., Zeminski, J., Abramowitch, S. D., Saw, S. S., and Fenwick, J. A., 2000, "Injury and Repair of Ligaments and Tendons," Annu. Rev. Biomed. Eng., **2**, pp. 83–118.
[3] Abramowitch, S. D., Clineff, T. D., Withrow, J. D., Papageorgiou, C. D., and Woo, S. L., 1999, "The Quasilinear Viscoelastic Properties of the Healing Goat Medial Collateral Ligament: An Experimental & Analytical Approach," 23rd Annual Meeting of the American Society of Biomechanics, Pittsburgh, Pennsylvania.
[4] Atkinson, T. S., Ewers, B. J., and Haut, R. C., 1999, "The Tensile and Stress Relaxation Responses of Human Patellar Tendon Varies With Specimen Cross-Sectional Area," J. Biomech., **32**, pp. 907–914.
[5] Atkinson, T. S., Haut, R. C., and Altiero, N. J., 1997, "A Poroelastic Model That Predicts Some Phenomenological Responses of Ligaments and Tendons," ASME J. Biomech. Eng., **119**, p. 400.
[6] Butler, S. L., Kohles, S. S., Thielke, R. J., Chen, C., and Vanderby, R., Jr., 1997, "Interstitial Fluid Flow in Tendons or Ligaments: A Porous Medium Finite Element Simulation," Med. Biol. Eng. Comput., **35**, pp. 742–746.
[7] Weiss, J. A., and Gardiner, J. C., 2001, "Computational Modeling of Ligament Mechanics," Crit. Rev. Biomed. Eng., **29**, pp. 303–371.
[8] Yamamoto, E., Hayashi, K., and Yamamoto, N., 1999, "Mechanical Properties of Collagen Fascicles From the Rabbit Patellar Tendon," ASME J. Biomech. Eng., **121**, pp. 124–131.
[9] Yin, L., and Elliott, D. M., 2004, "A Biphasic and Transversely Isotropic Mechanical Model for Tendon: Application to Mouse Tail Fascicles in Uniaxial Tension," J. Biomech., **37**, pp. 907–916.
[10] Miyazaki, H., and Kozaburo, H., 1999, "Tensile Tests of Collagen Fibers Obtained From the Rabbit Patellar Tendon," Biomed. Microdevices, **2**, pp. 151–157.
[11] Svensson, R. B., Hassenkam, T., Hansen, P., and Peter Magnusson, S., "Viscoelastic Behavior of Discrete Human Collagen Fibrils," J. Mech. Behav. Biomed. Mater., **3**, pp. 112–115.
[12] Armstrong, C. G., Lai, W. M., and Mow, V. C., 1984, "An Analysis of the Unconfined Compression of Articular Cartilage," ASME J. Biomech. Eng., **106**, pp. 165–173.
[13] Cohen, B., Lai, W. M., and Mow, V. C., 1998, "A Transversely Isotropic Biphasic Model for Unconfined Compression of Growth Plate and Chondroepiphysis," ASME J. Biomech. Eng., **120**, pp. 491–496.
[14] Diamant, J., Keller, A., Baer, E., Litt, M., and Arridge, R. G., 1972, "Collagen; Ultrastructure and Its Relation to Mechanical Properties as a Function of Ageing," Proc. R. Soc. London B Biol. Sci., **180**, pp. 293–315.
[15] Kastelic, J., Galeski, A., and Baer, E., 1978, "The Multicomposite Structure of Tendon," Connect Tissue Res., **6**, pp. 11–23.
[16] Rigby, B. J., Hirai, N., Spikes, J. D., and Eyring, H., 1959, "The Mechanical Properties of Rat Tail Tendon," J. Gen. Physiol., **43**, pp. 265–283.
[17] Screen, H. R. C., Bader, D. L., Lee, D. A., and Shelton, J. C., 2004, "Local Strain Measurement Within Tendon," Strain, **40**, pp. 157–163.
[18] Screen, H. R. C., and Cheng, V. W. T., 2007, "The Micro-structural Strain Response of Tendon," J. Materi. Sci., **19**, pp. 1–2.
[19] Lujan, T. J., Underwood, C. J., Jacobs, N. T., and Weiss, J. A., 2009, "Contribution of Glycosaminoglycans to Viscoelastic Tensile Behavior of Human Ligament," J. Appl. Physiol., **106**, pp. 423–431.

[20] Bonet, J., and Wood, R., 1997, *Nonlinear Continuum Mechanics for Finite Element Analysis*, Cambridge University Press, Cambridge, England.
[21] Beatty, M. F., and Stalnaker, D. O., 1986, "The Poisson Function of Finite Elasticity," J. Appl. Mech., **53**, pp. 807–813.
[22] Weiss, J. A., 1994, "A Constitutive Model and Finite Element Representation for Transversely Isotropic Soft Tissues," *Bioengineering*, University of Utah, Salt Lake City.
[23] Wellen, J., Helmer, K. G., Grigg, P., and Sotak, C. H., 2004, "Application of Porous-Media Theory to the Investigation of Water ADC Changes in Rabbit Achilles Tendon Caused by Tensile Loading," J. Magn. Reson., **170**, pp. 49–55.
[24] Helmer, K. G., Nair, G., Cannella, M., and Grigg, P., 2006, "Water Movement in Tendon in Response to a Repeated Static Tensile Load Using One-Dimensional Magnetic Resonance Imaging," ASME J. Biomech. Eng., **128**, pp. 733–741.
[25] Hannafin, J. A., and Arnoczky, S. P., 1994, "Effect of Cyclic and Static Tensile Loading on Water Content and Solute Diffusion in Canine Flexor Tendons: An *In Vitro* Study," J. Orthop. Res., **12**, pp. 350–356.
[26] Lavagnino, M., Arnoczky, S. P., Kepich, E., Caballero, O., and Haut, R. C., 2008, "A Finite Element Model Predicts the Mechanotransduction Response of Tendon Cells to Cyclic Tensile Loading," Biomech. Model Mechanobiol., **7**, pp. 405–416.
[27] Albro, M. B., Chahine, N. O., Li, R., Yeager, K., Hung, C. T., and Ateshian, G. A., 2008, "Dynamic Loading of Deformable Porous Media Can Induce Active Solute Transport," J. Biomech., **41**, pp. 3152–3157.
[28] Lynch, H. A., Johannessen, W., Wu, J. P., Jawa, A., and Elliott, D. M., 2003, "Effect of Fiber Orientation and Strain Rate on the Nonlinear Uniaxial Tensile Material Properties of Tendon," ASME J. Biomech. Eng., **125**, pp. 726–731.
[29] Hewitt, J., Guilak, F., Glisson, R., and Vail, T. P., 2001, "Regional Material Properties of the Human Hip Joint Capsule Ligaments," J. Orthop. Res., **19**, pp. 359–364.
[30] LeRoux, M. A., and Setton, L. A., 2002, "Experimental and Biphasic FEM Determinations of the Material Properties and Hydraulic Permeability of the Meniscus in Tension," ASME J. Biomech. Eng., **124**, pp. 315–321.
[31] Elliott, D. M., Robinson, P. S., Gimbel, J. A., Sarver, J. J., Abboud, J. A., Iozzo, R. V., and Soslowsky, L. J., 2003, "Effect of Altered Matrix Proteins on Quasi-linear Viscoelastic Properties in Transgenic Mouse Tail Tendons," Ann. Biomed. Eng., **31**, pp. 599–605.
[32] Gupta, H. S., Seto, J., Krauss, S., Boesecke, P., and Screen, H. R., 2010, "In Situ Multi-level Analysis of Viscoelastic Deformation Mechanisms in Tendon Collagen," J. Struct. Biol., **169**, pp. 183–191.
[33] Reese, S. P., Maas, S. A., and Weiss, J. A., 2010, "Micromechanical Models of Helical Superstructures in Ligament and Tendon Fibers Predict Large Poisson's Ratios," J. Biomech., **43**, pp. 1394–1400.
[34] Yahia, L. H., and Drouin, G., 1989, "Microscopical Investigation of Canine Anterior Cruciate Ligament and Patellar Tendon: Collagen Fascicle Morphology and Architecture," J. Orthop. Res., **7**, pp. 243–251.
[35] Vidal, D. C., 2003, "Image Analysis of Tendon Helical Superstructure Using Interference and Polarized Light Microscopy," Micron, **34**, pp. 423–432.
[36] Vidal Bde, C., and Mello, M. L., 2009, "Structural Organization of Collagen Fibers in Chordae Tendineae As Assessed by Optical Anisotropic Properties and Fast Fourier Transform," J. Struct. Biol., **167**, pp. 166–175.
[37] Vidal Bde, C., 1995, "Crimp as Part of a Helical Structure," C. R. Acad. Sci. III, **318**, pp. 173–178.
[38] DiSilvestro, M. R., and Suh, J. K., 2001, "A Cross-Validation of the Biphasic Poroviscoelastic Model of Articular Cartilage in Unconfined Compression, Indentation, and Confined Compression," J. Biomech., **34**, pp. 519–525.
[39] DiSilvestro, M. R., Zhu, Q., and Suh, J. K., 2001, "Biphasic Poroviscoelastic Simulation of the Unconfined Compression of Articular Cartilage: II—Effect of Variable Strain Rates," ASME J. Biomech. Eng., **123**, pp. 198–200.
[40] Huang, C. Y., Mow, V. C., and Ateshian, G. A., 2001, "The Role of Flow-Independent Viscoelasticity in the Biphasic Tensile and Compressive Responses of Articular Cartilage," ASME J. Biomech. Eng., **123**, pp. 410–417.
[41] Huang, C. Y., Soltz, M. A., Kopacz, M., Mow, V. C., and Ateshian, G. A., 2003, "Experimental Verification of the Roles of Intrinsic Matrix Viscoelasticity and Tension-Compression Nonlinearity in the Biphasic Response of Cartilage," ASME J. Biomech. Eng., **125**, pp. 84–93.
[42] Mak, A. F., 1986, "Unconfined Compression of Hydrated Viscoelastic Tissues: A Biphasic Poroviscoelastic Analysis," Biorheology, **23**, pp. 371–383.